PERIODICA POLYTECHNICA SER. MECH. ENG. VOL. 36, NO. 2, PP. 111-123 (1992)

DETERMINATION OF AERODYNAMIC CHARACTERISTICS OF AN AIR SLIDE OF DOUBLE AIR SPACE (PART TWO)

L. KOVÁCS and S. VÁRADI

Department of Hydraulic Machines
Technical University of Budapest

Received: August 28, 1992

Abstract

A method will be presented for calculating aerodynamic characteristics of air slides with lower distribution space and upper collection space, or operating by suction. Solving equations for aerodynamic parameters by the Runge-Kutta method yields longitudinal distribution of velocity and pressure of air flowing through the distribution layer, as well as of air flowing in the distribution (collection) space along the air slide.

This computation method helps plotting of 'characteristic curve' of the duct; its intersection with the characteristic curve of the fan is the operating point.

Keywords: conveying, air slide conveying.

Introduction

Writing mathematical-physical model for determining velocity and pressure distribution in a duct of double air space, as well as of longitudinal velocity distribution of fluidizing air flowing across the air distribution layer, involves the following simplifying conditions:

— Omitting the velocity profile variation in the air distribution and collection space of the air slide, only mean velocity is reckoned with.
— In writing pressure drop of air flowing through the air distribution layer, resistance of the material layer over the air distribution layer is omitted. This involves no significant error, since in designing the duct, resistance of the distribution layer is taken as 6 to 15 times the material layer resistance. It is, of course, feasible to reckon with a distribution layer with a resistance increased by that of the material layer of depth m_0 flowing along the duct, considered as constant at a fair approximation.
— Duct sidewalls are mostly trilaterally confined by metal sheets. For the lower duct, the fourth side is the distribution layer, while for the upper duct, the flowing material layer. Duct resistance is reckoned

with as if the duct were made of a wall of the same quality on all four sides.

— Effect of the displacement of material layer on the air distribution layer, and variation of material layer depth m_0 are omitted.

— State change of air flowing in the duct is approximated by isothermal state change.

The Lower Air Distribution Duct

Continuity equation for the checking surface marked in the elementary duct length cut out at x of the air slide in *Fig. 1:*

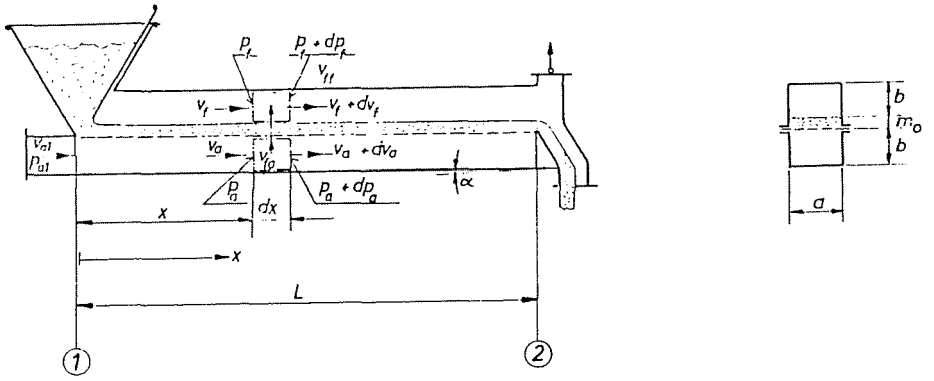

Fig. 1. Sketch of the air slide with closed upper air space

$$(v_a + \mathrm{d}v_a)ab(\varrho_a + \mathrm{d}\varrho_a) - v_a ab\varrho_a + v_{fa}\varrho_a a\mathrm{d}x = 0\,. \tag{1}$$

After possible reductions, *Eq.* (1) becomes:

$$\mathrm{d}x = -\frac{b}{\varrho_a v_{fa}}\mathrm{d}(\varrho_a v_a)\,. \tag{2}$$

Pressure drop of air flowing through the air distribution layer, may be written as follows:

$$\Delta p = p_a - p_f = k\varrho_a v_{fa} = k\varrho_f v_{ff}\,. \tag{3}$$

Utilizing parameters listed below:

$$x^* = \frac{x}{L}; \qquad b^* = \frac{b}{L}; \qquad v_a^* = \frac{v_a}{v_{a1}}; \qquad v_f^* = \frac{v_f}{v_{a1}}; \qquad v_{fa}^* = \frac{v_{fa}}{v_{a1}};$$

$$v_{ff}^* = \frac{v_{ff}}{v_{a1}}; \qquad p_a^* = \frac{p_a}{p_0}; \qquad p_f^* = \frac{p_f}{p_0}; \qquad \varrho_a^* = \frac{\varrho_a}{\varrho_0}; \qquad \varrho_f^* = \frac{\varrho_f}{\varrho_0}.$$

Eq. (3) may be written in non-dimensional form as:

$$\pi_1(p_a^* - p_f^*) = \varrho_a^* v_{fa}^* . \tag{4}$$

Using *Eq.* (4), *Eq.* (2) in non-dimensional form becomes:

$$\mathrm{d}x^* = -\frac{b}{\pi_1} \frac{\mathrm{d}(\varrho_a^* v_a^*)}{p_a^* - p_f^*} . \tag{5}$$

Applying the momentum theorem, it may be written:

$$p_a ab - (p_a + \mathrm{d}p_a)ab - \mathrm{d}F_{ra} =$$

$$= (v_a + \mathrm{d}v_a)(\varrho_a + \mathrm{d}\varrho_a)(v_a + \mathrm{d}v_a)ab - v_a \varrho_a v_a ab + v_{fa} \varrho_a a \,\mathrm{d}x\, v_a . \tag{6}$$

In the last term of the right-hand side of *Eq.* (6), elementary air mass flow through the elementary distribution layer:

$$\mathrm{d}\dot{m} = v_{fa} a \,\mathrm{d}x\, \varrho_a . \tag{7}$$

Thereby component in direction x of the momentum of air leaving elementary surface $a\mathrm{d}x$ is approximated as:

$$\mathrm{d}I_x \cong \mathrm{d}\dot{m} v_a = v_{fa} a \,\mathrm{d}x\, \varrho_a v_a . \tag{8}$$

In *Eq.* (6):

$$\mathrm{d}F_{ra} = \frac{\lambda}{2d_h} \varrho_a v_a^2 ab \,\mathrm{d}x . \tag{9}$$

Assuming isothermal state change leads to:

$$\frac{p_a}{\varrho_a} = \frac{p_0}{\varrho_0} = k_1 \tag{10}$$

and

$$\mathrm{d}p_a = k_1 \mathrm{d}\varrho_a . \tag{11}$$

Making use of continuity, momentum theorem (and *Eqs* (10) and (11)), after some transformations, for the lower air distribution duct the non-dimensional equation

$$\frac{\mathrm{d}p_a^*}{\mathrm{d}(\varrho_a^* v_a^*)} = \frac{\dfrac{\lambda(\mathrm{Re})b^*}{d_h^*} \dfrac{\pi_2}{\pi_1} \dfrac{(\varrho_a^* v_a^*)^2}{p_a^*(p_a^* - p_f^*)} - 2\pi_2 \dfrac{(\varrho_a^* v_a^*)}{p_a^*}}{1 - 2\pi_2 \dfrac{(\varrho_a^* v_a^*)^2}{p_a^{*2}}} \tag{12}$$

results.

The Upper Collecting Duct

In *Fig. 2*, the control surface has been specially marked. With the indicated velocities, continuity equation in direction y becomes:

$$v_{fa}\varrho_a = v_{ff}\varrho_f\,. \tag{13}$$

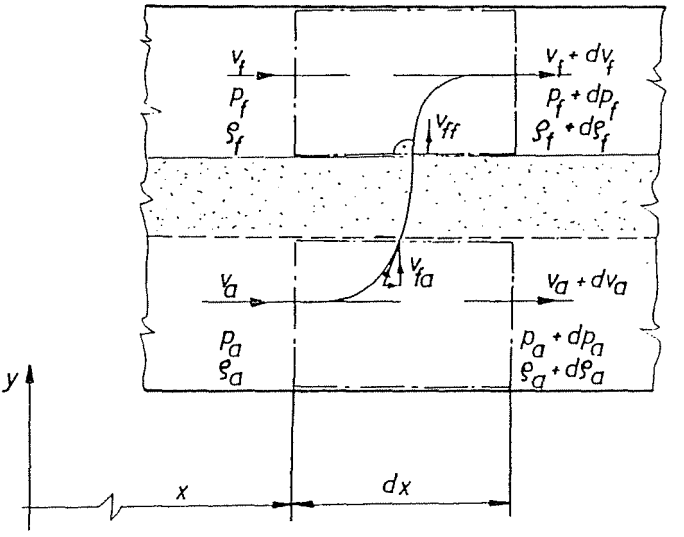

Fig. 2. Checking surface at a duct section with coordinate x

While in direction x:

$$(v_f + \mathrm{d}v_f)(\varrho_f + \mathrm{d}\varrho_f)ab - v_f\varrho_f ab - v_{ff}\varrho_f\, a\,\mathrm{d}x = 0\,. \tag{14}$$

Taking *Eq.* (13) into consideration, continuity equation in non-dimensional form:

$$\mathrm{d}x^* = b^*\frac{\mathrm{d}(\varrho_f^* v_f^*)}{(\varrho_f^* v_{ff}^*)} = b^*\frac{\mathrm{d}(\varrho_a^* v_a^*)}{(\varrho_a^* v_{fa}^*)}\,. \tag{15}$$

Utilizing *Eq.* (4), *Eq.* (15) can also be written as:

$$\mathrm{d}x^* = \frac{b^*}{\pi_1}\frac{\mathrm{d}(\varrho_f^* v_f^*)}{p_a^* - p_f^*}\,. \tag{16}$$

Continuity equation (16) differs from *Eq.* (5) only by sign, as expected.

In writing the momentum theorem, it has to be taken into consideration that — according to [1] — flow line of air flowing through the distribution layer and entering the upper checking surface is such that component in direction x of air velocity is here negligible.

Accordingly, here velocity is about parallel to the y-axis.

Now, the momentum theorem becomes:

$$p_f ab - (p_f + \mathrm{d}p_f)ab - \mathrm{d}F_{rf} =$$

$$= (v_f + \mathrm{d}v_f)(\varrho_f + \mathrm{d}\varrho_f)(v_f + \mathrm{d}v_f)ab - v_f \varrho_f v_f \, ab \,. \tag{17}$$

Reduction and some rearrangement of the equations yields for the upper duct the non-dimensional equation:

$$\frac{\mathrm{d}p_f^*}{\mathrm{d}(\varrho_f^* v_f^*)} = \frac{\dfrac{\lambda(\mathrm{Re})b^*}{d_h^*}\,\dfrac{\pi_2}{\pi_1}\,\dfrac{(\varrho_f^* v_f^*)^2}{p_f^*(p_a^* - p_f^*)} + 4\pi_2\,\dfrac{(\varrho_f^* v_f^*)}{p_f^*}}{1 - 2\pi_2\,\dfrac{(\varrho_f^* v_f^*)^2}{p_f^{*2}}} \,. \tag{18}$$

For air flows in the lower, and upper air spaces of the double duct, differential *Eqs.* (12), and (18), resp., result. Knowing initial conditions, equations can be solved by the Runge-Kutta method. For $x^* = 1$, (at 2 in *Fig. 1*) initial conditions are:

For the lower duct:

$$p_a^* = p_{a2}^* \,; \qquad \varrho_{a2}^* v_{a2}^* = 0 \,. \tag{19}$$

For the upper duct:

$$p_{f2}^* = 1 \,; \qquad \varrho_{f2}^* v_{f2}^* = \varrho_{a1}^* v_{a1}^* \,. \tag{20}$$

Velocity v_{a1} involved in π_2 being unknown at the beginning of computation, it has to be taken by assessing. Program-borne iteration approximates the assumed velocity until equality between mass flows entering through cross section '1' and leaving through cross section '2' is met, within the specified margin of error. For the computation, also the v_{ff} value at $x^* = 1$ has to be assumed, fitting fluidization velocity of the conveyed material. Thereafter the Δp_{a2}^* value in *Eq.* (19) can be determined, in knowledge of the constant characteristic of the air distribution layer.

Longitudinal pressure variations in the lower and upper air spaces of a double duct are seen in *Fig. 3.* Intercept between the two curves —

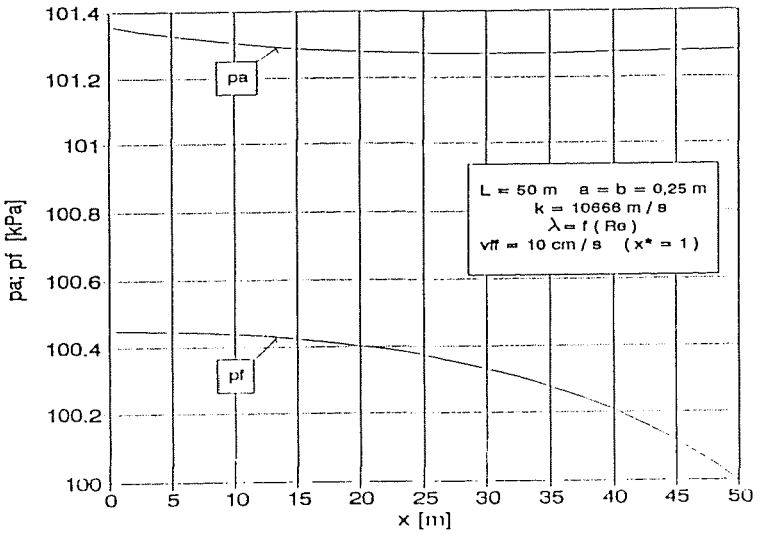

Fig. 3. Longitudinal pressure distribution in the duct

difference between pressures below and above the air distribution layer — is proportional to the mass flow across the air distribution layer.

Longitudinal variations of velocities v_{fa} and v_{ff} of flow through distribution layer of different resistances are seen in *Fig. 4*. For every curve, $v_{ff} = 10\,\text{cm/s}$ at $x^* = 1$. The greatest variation occurs — as expected — for the distribution layer with the least resistance. Here velocity $v_{ff} = 10\,\text{cm/s}$ in about the first third of the duct drops to $v_{ff} = 6.7\,\text{cm/s}$.

Longitudinal velocity variations in air spaces of the lower and of the upper duct are seen in *Fig. 5*. The two curves are not quite rectilinear.

Set of characteristic curves of a double duct $L = 50\,\text{m}$ long is seen in *Fig. 6*, with the constant parameters of the distribution layer, and the fluidization velocity v_{ff} at $L = 50\,\text{m}$ as parameters. Also characteristic curve of a fan has been plotted. Intersection of characteristic curves of fan and duct is the operating point where fan and duct can interact.

Duct without Lower Distribution Space. Duct Operating by Suction

Duct operating by suction in *Fig. 7* differs from that in *Fig. 1* by having no duct below the air distribution layer, that is thereby directly contacting the atmospheric space. Suction fan joins the collection duct at the top.

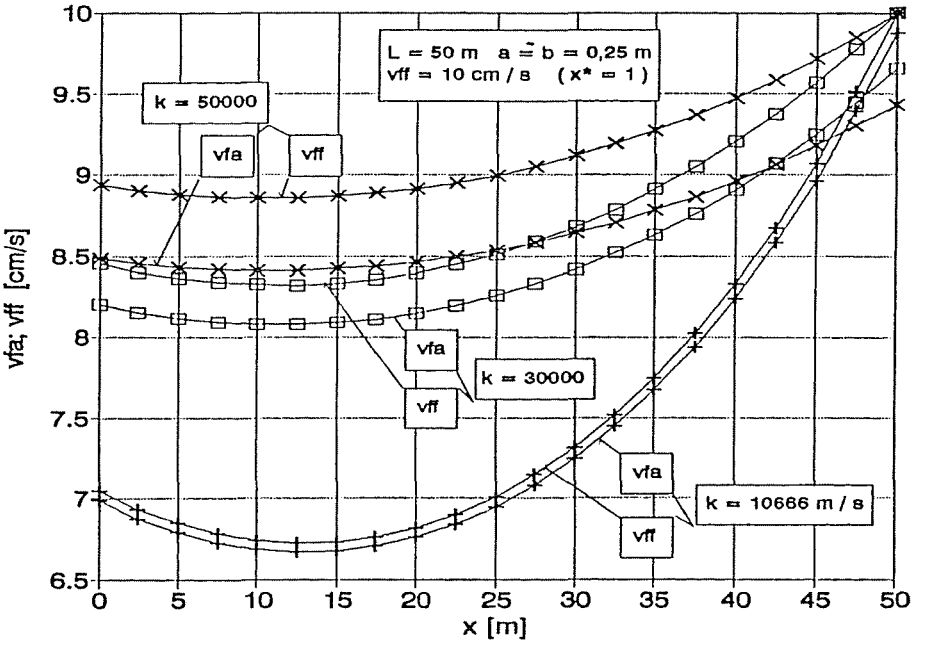

Fig. 4. Velocity variation of air flowing through distribution layers of different resistances

A duct of this arrangement exhibits a simpler construction and an easier changing of the distribution layer.

Among equations deduced for the double duct, *Eq.* 18 for the upper duct lends itself to determine aerodynamic parameters of the suction duct.

For the outlined duct, pressure under the fabric is approximately constant along the duct, and its value equals the atmospheric pressure p_0. Hence, substituting

$$p_a^* = 1$$

into *Eq.* (18) yields for aerodynamic characteristics of the duct operating by suction:

$$\frac{\mathrm{d}p_f^*}{\mathrm{d}(\varrho_f^* v_f^*)} = -\frac{\dfrac{\lambda(\mathrm{Re})b^*}{d_h^*}\dfrac{\pi_2}{\pi_1}\dfrac{(\varrho_f^* v_f^*)^2}{p_f^*(1-p_f^*)} + 4\pi_2\dfrac{(\varrho_f^* v_f^*)}{p_f^*}}{1 - 2\pi_2\dfrac{(\varrho_f^* v_f^*)^2}{p_f^{*2}}}. \tag{21}$$

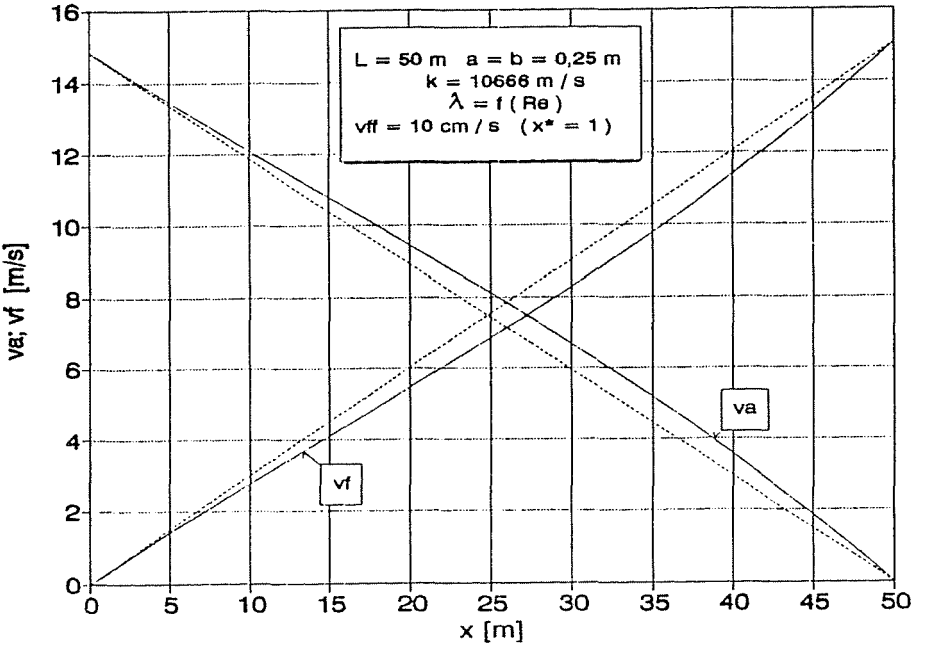

Fig. 5. Longitudinal velocity variation in lower and upper air spaces of the duct

Making use of continuity equation (16), *Eq.* (21) may be solved by the Runge-Kutta method. Initial condition at $x^* = 0$ (at '1' in the diagram):

$$\Delta p_f^* = \Delta p_{f1}^* ; \qquad \varrho_{f1}^* v_{f1}^* = 0 .$$

To calculate $\Delta p_f^* = \Delta p_{f1}^*$, the v_{ff} value at $x^* = 0$ has to be assumed, fitting fluidization velocity of the conveyed matter. Having assumed the velocity, the Δp_{f1}^* value can be determined in knowledge of the constant characteristic of the air distribution layer.

Pressure variation vs. suction duct length is seen in *Fig. 8*. At the duct inlet, at $x = 0$, pressure is lower by Δp_{f1} belonging to $v_{ff} = 10\,\mathrm{cm/s}$ than the atmospheric pressure. The most of depression is at the duct end at $x = 50\,\mathrm{m}$, where pressure $p_{f2} = 97550\,\mathrm{Pa}$.

Flow velocities v_{fa} and v_{ff} at entering and at leaving, resp., the air distribution layer have been plotted in *Fig. 9*. As against similar curves for the double duct, these curves are seen not to have minimum. This may be attributed to that curve $p_f = f(x)$ in *Fig. 8* has no minimum. In the upper collector duct, flow is of 'confusor' type, this pressure drop is furthered by the duct loss responsible for the important variation of velocity v_{ff} (v_{fa}). This velocity grows from $v_{fa1} = 10\,\mathrm{cm/s}$ at the duct inlet to $v_{fa2} = 19.4\,\mathrm{cm/s}$ at the duct end, impairing the duct operation.

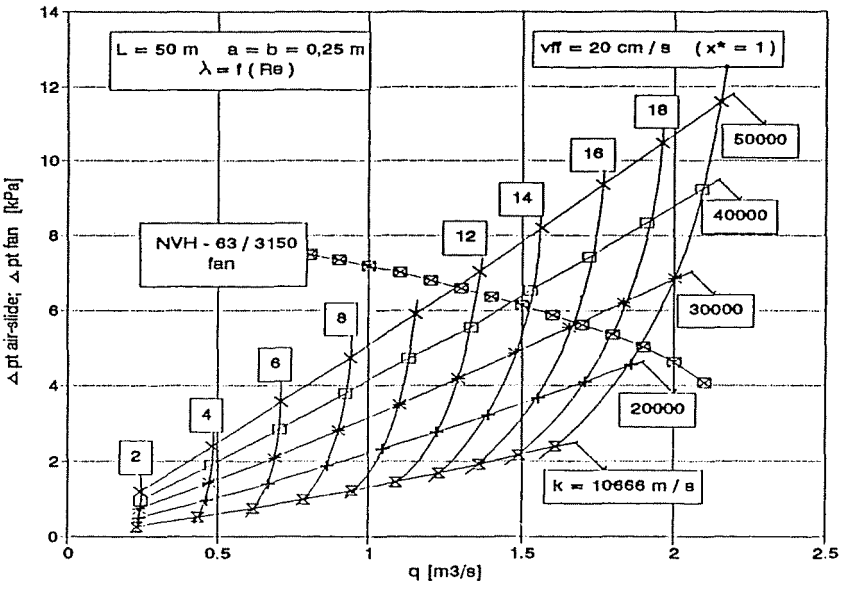

Fig. 6. Set of characteristic curves of the double air slide; with the constant characteristic of the distribution layer, and the fluidization velocity at the boundary as parameters

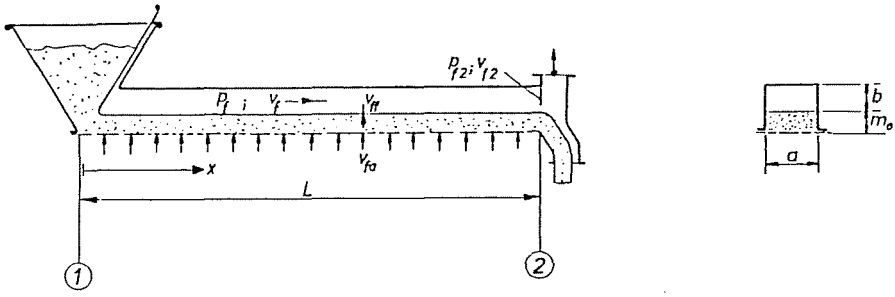

Fig. 7. Sketch of a duct operating by suction, with infinite lower air space

Variation of velocity v_f along the duct vs. duct length has been plotted in *Fig. 10.* Velocity increases from the initial $v_{f1} = 0$ to $v_{f2} = 25.4$ m/s at the duct end, as read off the diagram.

A set of characteristic curves for a duct operating by suction, without lower air distribution space, is seen in *Fig. 11,* again with constant parameters of the distribution layer, and the fluidization velocity v_{ff} at the

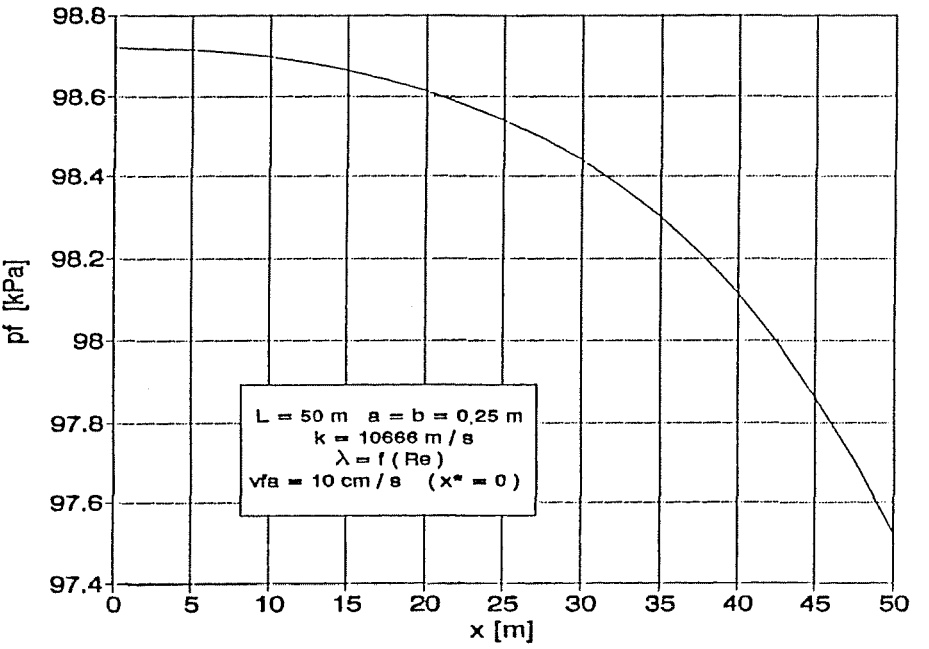

Fig. 8. Longitudinal pressure distribution in a suction duct

boundary ($x^* = 0$) as parameters. Also the characteristic curve of a fan has been plotted, for the sake of determining the operating point.

Legend

a	[m]	duct width
$A = ab$	[m^2]	duct cross section
b	[m]	duct depth
$b^* = \frac{b}{L}$	[–]	non-dimensional depth
$d_h = \frac{4A}{K}$	[m]	hydraulic diameter
F_r	[N]	friction force
k	[m/s]	constant characteristic of the distribution layer
$K = 2(a + b)$	[m]	perimeter of the air distribution space (collecting space)
$\pi_1 = \frac{p_0}{k\varrho_0 v_{a1}}$	[–]	constant

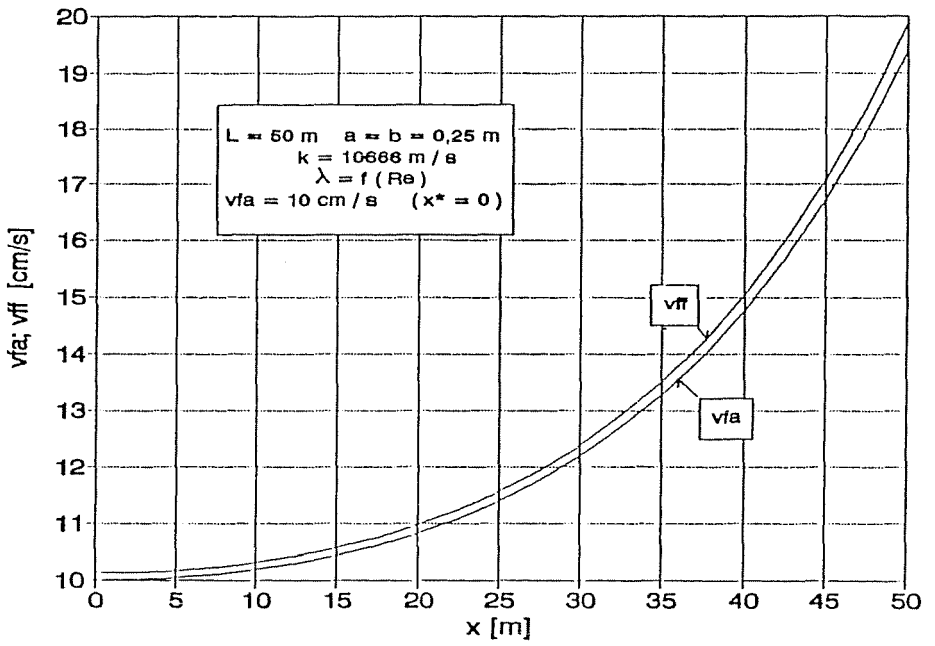

Fig. 9. Longitudinal distribution of flow velocity of air flowing across the distribution layer in a suction duct

$\pi_2 = \frac{\varrho_0 v_{a1}^2}{2p_0}$	[–]	constant
L	[m]	duct length
m_0	[m]	material layer depth
p_a	[Pa]	pressure in the lower duct space
p_0	[Pa]	atmospheric pressure
p_f	[Pa]	pressure in the upper duct space
$p_a^* = \frac{p_a}{p_0}$	[–]	non-dimensional pressure
$p_f^* = \frac{p_f}{p_0}$	[–]	non-dimensional pressure
$\Delta p = p_a - p_f$	[Pa]	pressure drop of air passing through the air distribution layer
$\Delta p^* = \frac{\Delta p}{p_0} = p_a^* - p_f^*$	[–]	non-dimensional pressure drop
$\dot{m}$	[kg/s]	air mass flow
q	[m^3/s]	air volume flow
$\mathrm{Re} = \frac{d_h v}{\nu}$	[–]	Reynolds number
v_a; v_f	[m/s]	air velocities in lower and upper distribution

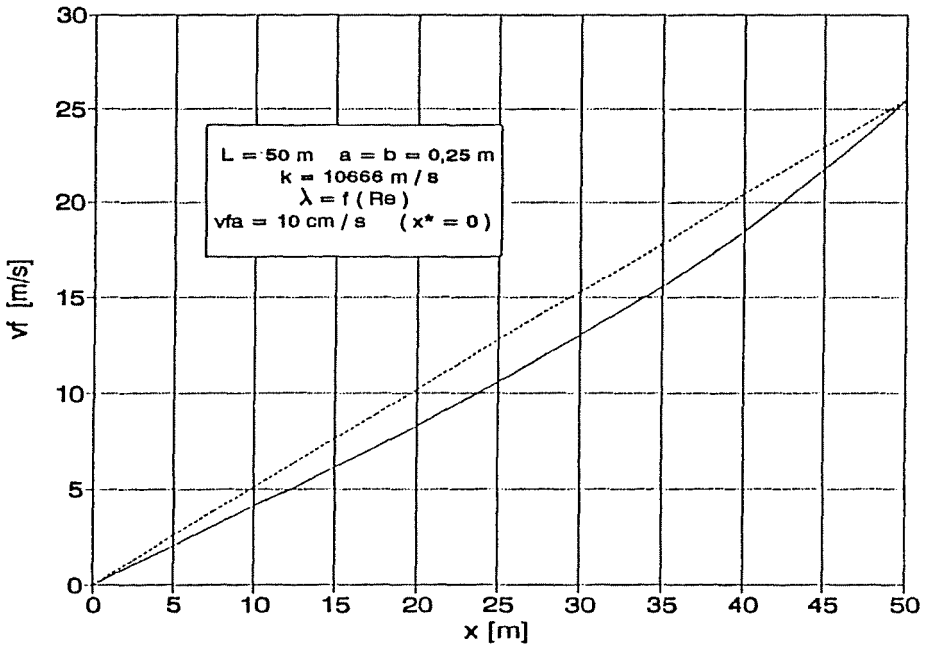

Fig. 10. Longitudinal velocity variation in a duct operating by suction

		and collection ducts, respectively
$v_a^* = \frac{v_a}{v_{a1}}$	[–]	non-dimensional velocity in the lower duct
$v_f^* = \frac{v_f}{v_{a1}}$	[–]	non-dimensional velocity in the upper duct
v_{fa}	[m/s]	'fluidization' velocity of air entering the distribution layer
$v_{fa}^* = \frac{v_{fa}}{v_{a1}}$	[–]	non-dimensional 'fluidization' velocity
v_{ff}	[m/s]	'fluidization' velocity of air leaving the distribution layer
$v_{ff}^* = \frac{v_{ff}}{v_{a1}}$	[–]	non-dimensional 'fluidization' velocity
x	[m]	coordinate
$x^* = \frac{x}{L}$	[–]	non-dimensional coordinate
y	[m]	coordinate
λ	[–]	friction factor
ϱ_a; ϱ_f	[kg/m^3]	air density in the lower (upper) duct
ϱ_0	[kg/m^3]	air density in normal state

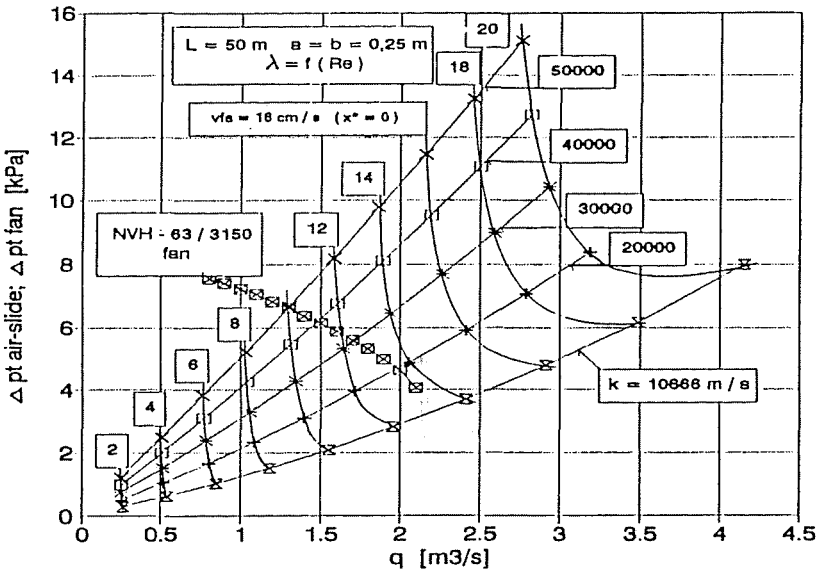

Fig. 11. Set of characteristic curves of a suction air slide without lower air distribution space; with the constant characteristic of the distribution layer, and the fluidization velocity at the boundary layer

$\varrho_a^* = \frac{\varrho_a}{\varrho_0}$ [–] non-dimensional density in the lower duct

$\varrho_f^* = \frac{\varrho_f}{\varrho_0}$ [–] non-dimensional density in the upper duct

Subscripts

1 duct inlet
2 duct outlet
fa 'fluidizing' air entering the distribution layer
ff 'fluidizing' air leaving the distribution layer
a lower duct space
f upper duct space

References

KOVÁCS, L. – VÁRADI, S.: Longitudinal Pressure Variation in the Lower Air Distribution Space in an Air-Slide Conveyor with Open Top Air Space. *Periodica Polytechnica Ser. Mechanical Engineering*, Vol. 36, No. 1.pp.

KÓSA, L. – VERBA, A. – TALLIÁN, A.: Berechnung der Treibkraft in aerokinetischer Rinne. Second Conference on Pneumatic Transport. March 1978. Pécs, Hungary.

Address:

Dr. László KOVÁCS
Dr. Sándor VÁRADI
Department of Hydraulic Machines
Technical University of Budapest
H–1521 Budapest